Virology 537 (2019) 36–44

Contents lists available at ScienceDirect

Virology

journal homepage: www.elsevier.com/locate/virology

Efficient pre-catalytic conformational change of reverse transcriptases from SAMHD1 non-counteracting primate lentiviruses during dNTP incorporation

Si'Ana A. Coggins[a], Jessica M. Holler[a], Jason T. Kimata[b], Dong-Hyun Kim[c], Raymond F. Schinazi[a], Baek Kim[a,c,d,*]

[a] Department of Pediatrics, School of Medicine, Emory University, Atlanta, GA, 30322, USA
[b] Department of Molecular Virology and Microbiology, Baylor College of Medicine, Houston, 77030, Texas, USA
[c] College of Pharmacy, Kyung Hee University, Seoul, 04427, South Korea
[d] Children's Healthcare of Atlanta, Atlanta, 30322, USA

ARTICLE INFO

Keywords:
Reverse transcriptase
Lentiviruses
SAMHD1
dNTPs
Macrophages
Conformational change
Vpx
Vpr

ABSTRACT

Unlike HIV-1, HIV-2 and some SIV strains replicate at high dNTP concentrations even in macrophages due to their accessory proteins, Vpx or Vpr, that target SAMHD1 dNTPase for proteasomal degradation. We previously reported that HIV-1 reverse transcriptase (RT) efficiently synthesizes DNA even at low dNTP concentrations because HIV-1 RT displays faster pre-steady state k_{pol} values than SAMHD1 counteracting lentiviral RTs. Here, since the k_{pol} step consists of two sequential sub-steps post dNTP binding, conformational change and chemistry, we investigated which of the two sub-steps RTs from SAMHD1 non-counteracting viruses accelerate in order to complete reverse transcription in the limited dNTP pools found in macrophages. Our study demonstrates that RTs of SAMHD1 non-counteracting lentiviruses have a faster conformational change rate during dNTP incorporation, supporting that these lentiviruses may have evolved to harbor RTs that can efficiently execute the conformational change step in order to circumvent SAMHD1 restriction and dNTP depletion in macrophages.

1. Introduction

During the course of its pathogenesis, HIV-1 infects both activated/dividing CD4$^+$ T cells and terminally differentiated/nondividing myeloid cells such as macrophages and microglia (Jamburuthugoda et al., 2006; Diamond et al., 2004; Weissman et al., 1997; Swanstrom et al., 2018). While activated CD4$^+$ T cells support robust HIV-1 replication kinetics and undergo rapid cell death upon infection, HIV-1 replication kinetics in macrophages is greatly suppressed. HIV-1 infected myeloid cells display long cell survival, leading to the persistent production of low levels of HIV-1, particularly in the brain (Bejarano et al., 2018; Williams and Hickey, 2002). A series of recent studies revealed that the observed suppressed HIV-1 replication kinetics in myeloid cells is due to host SAM domain and HD domain containing protein 1 (SAMHD1) which is a dNTP triphosphohydrolase (dNTPase) that depletes the dNTP substrates of reverse transcriptases (RT) in macrophages (Amie et al., 2013; Goldstone et al., 2011). However, some SIV strains replicate rapidly even in macrophages. The fast replication capability of these SIV strains is due to their accessory protein, viral protein X (Vpx) (Hrecka et al., 2011; Laguette et al., 2011), which is a gene duplication product of another viral accessory protein, viral protein R (Vpr) (Sharp et al., 1996; Etienne et al., 2013). Lentiviral Vpx directly binds to host SAMHD1 protein and induces the E3-ligase mediated proteasomal degradation of SAMHD1 (Hrecka et al., 2011; Ahn et al., 2012; Srivastava et al., 2008). Less abundant SAMHD1 leads to the elevation of cellular dNTP concentrations in macrophages and the acceleration of reverse transcription during the viral replication cycle (Lahouassa et al., 2012). Several studies demonstrated that this SAMHD1 degradation capability already existed among SIV strains that encode Vpr, but not Vpx, such as the SIVagm strains (Lim et al., 2012). These SIV strains use their Vpr proteins to counteract their host SAMHD1 via the same proteasomal degradation pathway hijacked by Vpx (Belzile et al., 2007; Hrecka et al., 2007). Importantly, while SAMHD1 sequence variations are observed among the many primate host species, Vpr/Vpx species specificity also recognizes host-specific SAMHD1 sequences for the proteasomal degradation (Fregoso et al., 2013; Schwefel et al., 2014).

Due to the presence of host SAMHD1, SAMHD1 non-counteracting lentiviruses such as HIV-1 replicate in limited dNTP pools during the infection of macrophages; conversely, SAMHD1 counteracting lentiviruses such as SIVmac239 replicate under abundant dNTP conditions

* Corresponding author. Center for Drug Discovery, Department of Pediatrics, School of Medicine, Emory University, 1760 Haygood Drive E432, Atlanta, GA, 30322, USA.
E-mail address: baek.kim@emory.edu (B. Kim).

https://doi.org/10.1016/j.virol.2019.08.010
Received 16 July 2019; Received in revised form 10 August 2019; Accepted 12 August 2019
Available online 14 August 2019

even in macrophages. We previously observed that SAMHD1 non-counteracting lentiviral RTs can efficiently synthesize DNA even at the low dNTP concentrations found in macrophages. This suggests that the efficient DNA synthesis capability of SAMHD1 non-counteracting lentiviral RTs enables these lentiviruses to overcome SAMHD1-mediated viral restriction (Lenzi et al., 2014). The slower replication kinetics of HIV-1 compared to those of SAMHD1 counteracting strains such as HIV-2 and some SIVs, reveal that the potential RT-mediated mechanism to overcome low dNTP concentrations in macrophages is much less effective than Vpx/Vpr-mediated SAMHD1 degradation. However, this RT-mediated mechanism may enable HIV-1 to complete its reverse transcription step even in macrophages with limited dNTP pools. Pre-steady state kinetic analysis using a rapid quench instrument (Skasko et al., 2005; Lenzi et al., 2015) can simultaneously measure K_d (dNTP binding affinity) and k_{pol} (K_{conf} + K_{chem}), lending insight into the molecular activities and mechanisms of various enzymes. Employing the use of pre-steady state kinetic analyses, we previously reported that while SAMHD1 non-counteracting lentiviral RTs display faster rates of incorporation (k_{pol}) when compared to SAMHD1 counteracting lentiviral RTs, these polymerases share similar K_d values (Lenzi et al., 2015). This suggests that the faster k_{pol} values of the SAMHD1 non-counteracting lentiviral RTs allow these viruses to complete proviral DNA synthesis even at the low dNTP concentrations found in macrophages.

In this study, we investigated the pre-steady state kinetics and elemental effect of RTs from various SAMHD1 counteracting and non-counteracting primate lentivirus strains in order to understand the differential relationship between RT kinetics and host SAMHD1 proteins among these lentiviruses. It was demonstrated with many DNA polymerases (Mizrahi.V et al., 1985; Huang et al., 2018; Fiala and Suo, 2004; Zahurancik et al., 2013), including HIV-1 RT (Hsieh JC and Modrich, 1993), that (i) the K_{conf} step is the slowest/rate-limiting step during the pre-steady state dNTP incorporation reaction and (ii) the K_{chem} step is very rapid, indicating that the k_{pol} value is predominantly represented by the K_{conf} step ($k_{pol} \approx K_{conf}$). This conclusion was experimentally made by the absence of the phosphorothioate elemental effect when using dNTPαS substrates which contain sulfur instead of oxygen at the α-phosphate position of dNTP. During the incorporation of dNTPαS, the sulfur atom present on the alpha-phosphate of the substrate slows only the chemistry step (K_{chem}), a phenomenon defined as an elemental effect.

In this study, we determined the elemental effect of RTs from SAMHD1 non-counteracting SIV strains, SIVcpz and SIVgor, and RTs from SAMHD1 counteracting SIV strains, SIVagm 9063–2 and SIVmne CL8. Overall, our kinetic analysis explains how the RTs of the SAMHD1 non-counteracting lentiviruses mechanistically gained faster k_{pol} rates and how these lentiviruses became capable of circumventing SAMHD1-mediated restriction in order to complete proviral DNA synthesis even at the extremely low cellular dNTP concentrations found in nondividing macrophages.

2. Experimental procedures

Cells, plasmids and chemicals: The following full-length clones of various HIV-1 and SIV strains were obtained through the AIDS Reagent Program, Division of AIDS, NIAID, National Institutes of Health: HIV-1 94UG114.1 Non-infectious Molecular Clone from Drs. Beatrice Hahn and Feng Gao, and the UNAIDS Network for HIV Isolation and Characterization (cat# 4001) (Gao et al., 1998); HIV-1 94CY017.41 Non-infectious Molecular Clone from Drs. Stanley A. Trask, Feng Gao, Beatrice H. Hahn, and the Aaron Diamond AIDS Research Center (cat# 6175) (Gao et al., 2001); pSIV$_{gor}$CP2139 from Drs. Jun Takehisa, Matthias H. Kraus, and Beatrice H. Hahn (cat#11722) (Takehisa et al., 2009); SIV$_{CPZ}$TAN2.69 from Drs. Jun Takehisa, Matthias H. Kraus and Beatrice H. Hahn (Cat #11497) (Takehisa et al., 2007). A full-length molecular clone of SIVmne CL8 was previously constructed (Rudensey et al., 1995), while a full-length molecular clone of SIVagm 9063–2 was kindly provided by V. Hirsh (Hirsch et al., 1995) (National Institutes of Health, Bethesda, MD). The aforementioned molecular clones were used to clone the flag tagged Vpr genes of HIV-1 Ug and HIV-1 Cy into pCDNA3.1/hygro (+) (*Hind*III and *Xho*I, ThermoFisher) while the flag tagged Vpr genes of SIVgor, SIVcpz, and SIVagm 9063–2 were synthesized into pcDNA3.1/Hygro (+) by GenScript (Piscataway, NJ). Full length molecular clones were also used to clone the RT genes of HIV-1 Cy (Lenzi et al., 2014), HIV-1 Ug (Lenzi et al., 2014), SIVagm 9063–2 (Skasko et al., 2009), SIVgor, SIVcpz 2.69 into pET28a (*Nde*I and *Xho*I sites, Novagen) and SIVmneCL8 RT into pHis (*Nde*I and *Eco*RI). The following SAMHD1 proteins were synthesized into pLVX-IRES- mCherry with an N-terminal HA tag from NCBI Reference sequences NM_001280510.1 (chimpanzee) and NM_001279619.1 (gorilla). The hSAMHD1 gene encoded from the plasmid provided by Dr. Felipe Diaz-Griffero (Bhattacharya et al., 2016) was cloned into pLVX-IRES-mCherry with an N-terminal HA tag. African Green Monkey SAMHD1 haplotype IV in pLPCX was gifted from Dr. Michael Emerman (Spragg and Emerman, 2013) (Fred Hutchinson Cancer Research Center, Seattle, WA). Pigtail macaque SAMHD1 gene was amplified from pigtail macaque mRNAs and cloned into pcDNA3.1. Rhesus macaque SAMHD1 in pLenti was generously obtained from Dr. Nathaniel Landau (New York University, New York, NY). Also obtained from Dr. Nathaniel Landau were a plasmid expressing SIVmac251 proteins except Env (pSIV3 +Vpx) and pSIV3 with Vpx deletion (pSIV -Vpx) (Berger et al., 2011; Mangeot et al., 2000).

SAMHD1 degradation assay: The SAMHD1 degradation assay was conducted as previously reported (Fregoso et al., 2013; Spragg and Emerman, 2013; Mereby et al., 2018). Briefly, using polyethylenimine, 293T cells (2×10^6 cells) were co-transfected with a plasmid expressing host specific HA-tagged SAMHD1 proteins (0.1 μg) and a plasmid expressing either flag-tagged (SIVagm 9063–2) or HA-tagged (HIV-1 Cy, HIV-1 Ug, SIVgor, and SIVcpz) viral accessary proteins Vpx/Vpr or the entire proviral genome (SIVmne CL8) (2 μg). The cell lysates were prepared by sonication from the transfected cells at 48 h post transfection and western blots were performed to visualize not only HA-tagged primate SAMHD1 proteins using an anti-HA antibody, but also hSAMHD1 using *anti*-hSAMHD1 antibody. GAPDH was used for as a loading control. Vpr and Vpx proteins were visualized using anti-flag tag and anti-HA tag antibodies. The mean relative SAMHD1 levels were calculated by densitometry analysis and normalized to the GAPDH loading control. The ratios of the normalized SAMHD1 levels with and without viral protein expression were calculated for determining the SAMHD1 degradation efficiency.

RT protein expression and purification: All six N-terminal His-tagged RTs were expressed in *E. coli* BL21 Rosetta 2 DE3 (Millipore) and their p66/p66 homodimers were purified as described previously (Kim, 1997) with the following changes. For HIV-1 Cy and SIVagm 9063-2 RTs, clear lysate obtained through sonication was applied to His·Bind resin (Millipore) equilibrated with a binding buffer containing 0.5 M NaCl, 20 mM Tris-HCl pH 7.9, and 5 mM imidazole. The column was washed with 15 column volumes binding buffer prior to being eluted in 1 mL fractions by a solution containing 20 mM Tris-HCl pH 7.9, 0.5 M NaCl, and 1 M imidazole. Fractions containing the His tagged-p66/p66 were pooled and dialyzed for 16 h in a buffer containing 50 mM Tris-HCl pH 7.5, 200 mM NaCl, 1 mM EDTA, and 10% glycerol. The RTs then underwent an additional 3 h dialysis in a solution containing 50 mM Tris-HCl pH 7.5, 200 mM NaCl, 1 mM EDTA, 10% glycerol, and 1 mM DTT. Purification of HIV-1 Ug, SIVmne CL8, SIVgor, and SIVcpz 2.69 RTs required different binding, elution, and dialysis/storage buffers. The clear lysate of these RTs was loaded onto a His-resin bed equilibrated with binding buffer containing 40 mM Tris-HCl pH 7.5, 250 mM KCl, 5 mM $MgCl_2$, 5 mM beta-mercaptoethanol, 20 mM imidazole, and 10% glycerol. The proteins were eluted from the column using a solution containing 40 mM Tris-HCl pH 7.5, 250 mM KCl, 5 mM $MgCl_2$, 240 mM imidazole, and 10% glycerol before being dialyzed for 16 h in a buffer containing 50 mM Tris-HCl pH 7.5, 150 mM KCl,

0.25 mM EDTA, 1 mM beta-mercaptoethanol, and 20% glycerol. To examine the purity of the proteins, the dialyzed RTs were run on a 4–15% SDS-PAGE gel (BioRad) (Supplemental Fig. 1). All RTs were determined to have at least 95% purity and were flash frozen in liquid nitrogen prior to being stored at −80 °C for future use.

Pre-steady state kinetic analysis: To determine the active site concentration of the six RT proteins, we first performed pre-steady-state burst experiments using an RFQ-3 rapid quench-flow apparatus (KinTek Corporation). A^{32}P-labelled template:primer (T/P) was prepared by annealing a 5′-^{32}P-labelled 17mer primer (5′- CGCGCCGAA TTCCC GCT-3′, Integrated DNA Technologies) to a 3-fold excess of 40mer RNA template (5′-AAGCUUGGCUGCAGAAUAUUGCUAGCGGGAAUUCGGC GCG-3′, Integrated DNA Technologies). In burst experiments, 100 nM RT pre-bound to 300 nM T/P through a 10 min incubation at 37 °C was rapidly mixed with a solution containing 300 μM dATP, 10 mM $MgCl_2$, 50 mM Tris-HCl, pH 7.8 and 50 mM NaCl at 37 °C. The reactions were quenched at the following time points with EDTA: 0, 0.005, 0.01, 0.05, 0.1, 0.5, 1, 2, and 3 s. Reaction products were separated on 14% polyacrylamide/8 M urea gel, visualized using a PharosFX (Bio-Rad), and quantified with Image Lab Software (Bio-Rad). To determine the active site concentration of each purified RT, product formation was fit to the burst equation (Eq. (1)).

$$[Product] = A[1 - \exp(-k_{obs} \times t)] + (k_{ss} \times t) \quad \text{Eq. 1}$$

In this equation, A is the amplitude of the burst and reflects the concentration of enzyme that is in an active form, k_{obs} is the observed first-order burst rate for dNTP incorporation, and k_{ss} is the linear steady state rate constant (Lenzi et al., 2015; Kati et al., 1992; Reardon, 1992). Active site titrations were performed in triplicate for each lentiviral RT.

Finally, to determine the pre-steady state kinetic activity of the six RTs, we employed single turnover experiments. For these experiments, a^{32}P-labelled template:primer (T/P) was prepared by annealing a 5′-^{32}P-labelled 22mer primer (5′- CGCGCCGAATTCCCGC TAGCAA-3′, Integrated DNA Technologies) to a 3-fold excess of 40mer RNA template (5′-AAGCUUGGCUGCAGAAUAUUGCUAGCGGGAAUUCGGC GCG-3′, Integrated DNA Technologies). In single turnover experiments, 250 nM active RT enzyme pre-bound to 50 nM T/P was rapidly mixed with a solution containing 10 mM $MgCl_2$ and varying concentrations (1.6, 6.25, 12.5, 25, 50, and 100 μM) of either dTTP or dTTPαS substrate in the presence of 50 mM Tris-HCl, pH 7.8, and 50 mM NaCl. The reactions were quenched at various time points (0, 0.01, 0.03, 0.05, 0.1, 0.5, and 2 s) with 3 mM EDTA and visualized using the same methods as above. The amounts of product were quantified using ImageLab software and plotted as a function of time. The data were then fit to a single exponential equation (Eq. (2)).

$$[Product] = A\left(1 - e^{-k_{obs}t}\right) \quad \text{Eq. 2}$$

In which A is the amplitude of product formation, k_{obs} is the observed pre-steady state rate for dNTP incorporation, and t is time. Next, k_{obs} was plotted as a function of substrate concentration and fit to a non-linear regression curve equation (Eq. (3)).

$$k_{obs} = \frac{k_{pol}[dNTP]}{K_d + [dNTP]} \quad \text{Eq. 3}$$

In which k_{pol} is the maximum rate of dNTP incorporation and K_d is the equilibrium dissociation constant for the dNTP substrate (Johnson, 1995). Single turnover experiments were conducted in triplicate for both dTTP and dTTPαS substrates.

Elemental effect analysis: The elemental effect of each RT was determined using the following equation (Herschlag et al., 1991):

$$Elemental\ Effect = \frac{k_{pol}(dTTP)}{k_{pol}(dTTP\alpha S)} \quad \text{Eq. 4}$$

If this value exceeds 4, it can be concluded that there is elemental effect. If this value is ≤ 4, then there is no elemental effect present (Patel et al., 1991; Wong et al., 1991).

3. Results and discussion

Test for SAMHD1 degradation capability of SIV strains: While SAMHD1 non-counteracting HIV-1 replicates in the SAMHD1-mediated limited dNTP pools found in macrophages, SAMHD1 counteracting lentiviruses such as HIV-2 and some SIV strains replicate under abundant dNTP conditions even in macrophages (Yu XF et al., 1991; Hollenbaugh et al., 2016). We previously reported that unlike RTs from SAMHD1 counteracting lentiviruses, HIV-1 RTs efficiently synthesize DNA even in the low dNTP concentrations found in macrophages (Lenzi et al., 2014). This led us to hypothesize that the efficient DNA synthesis capability of the SAMHD1 non-counteracting HIV-1 RTs enables these viruses to complete proviral DNA synthesis even in the SAMHD1 mediated limited dNTP concentrations found in infected macrophages. Our follow-up pre-steady state kinetic analysis reported that the efficient DNA synthesis kinetics of HIV-1 RTs is due to their performing a faster k_{pol} step than SAMHD1 counteracting lentiviral RTs (Lenzi et al., 2015) - a kinetic event which occurs after the binding of dNTP substrate (K_d step) to the active site (Joyce, 2010).

In this study, since the k_{pol} step consists of two sequential sub-steps (Joyce, 2010): 1) a conformational step followed by a 2) chemistry step (Hsieh JC and Modrich, 1993; Kati et al., 1992), we investigated which of these two post dNTP binding sub-steps the RTs of the SAMHD1 non-counteracting primate lentiviruses accelerate in order to execute the faster k_{pol} step than the RTs of the SAMHD1 counteracting lentiviruses. This study aimed at mechanistically elucidating how these two groups of lentiviruses evolutionarily adapted to the largely different cellular dNTP concentrations found in their nondividing myeloid target cells. For this investigation, we employed RTs of four different SIV strains: SIVgor, SIVcpz, SIVagm 9063–2 and SIVmne CL8.

Many SIV strains from various primate species counteract the antiviral activity of SAMHD1 by targeting the host protein for E3-ligase dependent proteasomal degradation (Hrecka et al., 2011; Ahn et al., 2012; Lim et al., 2012; Belzile et al., 2007; Zhou et al., 2017). The mechanism of counteracting SAMHD1 via proteasomal degradation was initially found in SIV strains encoding Vpx [*i.e.* SIVsm (Laguette et al., 2011)], a protein which directly binds to SAMHD1 and recruits the host DDB1-CUL4-DCAF E3 ligase complex to induce the proteasomal degradation of SAMHD1 (Hrecka et al., 2011; Laguette et al., 2011; Srivastava et al., 2008). Later works demonstrated that this *anti*-SAMHD1 mechanism already existed even in some of SIV strains that do not encode Vpx. However, another accessary protein of these SIV strains, Vpr, is capable of inducing SAMHD1 degradation in these primate lentiviruses. This suggests that there was a splitting of *anti*-SAMHD1 function during the gene duplication of Vpr that appears to have created Vpx and two populations of Vpr: one that is able to counteract SAMHD1 and one that is not (Etienne et al., 2013; Fregoso et al., 2013). Therefore, we began by testing the SAMHD1 degradation activity of the four SIV strains (SIVgor, SIVcpz, SIVagm 9063–2, and SIVmne CL8) that we here investigated for their RT enzyme kinetics.

SIVcpz and SIVgor are considered to be the origin of HIV-1 (Sakai et al., 2016; D'Arc et al., 2015), and like HIV-1, these two SIV strains encode Vpr, but not Vpx. Since it was previously reported that as observed with HIV-1 strains, SIVcpz Vpr does not proteasomal degrade chimpanzee SAMHD1 (Lim et al., 2012), we first verified these results and tested whether SIVgor Vpr can induce the proteasomal degradation of gorilla SAMHD1. Additionally, we tested the capability of SIVmne CL8 and SIVagm 9063–2 to degrade their host SAMHD1 proteins. Due to the host SAMHD1-lentivirus specificity (Fregoso et al., 2013) including SAMHD1 sequence variations among the host species, we expressed SAMHD1 proteins from the specific host species related to each of primate lentiviruses used in this study: gorilla, chimpanzee, pig-tailed macaque, and African green monkey (haplotype IV) (Spragg and Emerman, 2013) for the SAMHD1 degradation assay (Fregoso et al.,

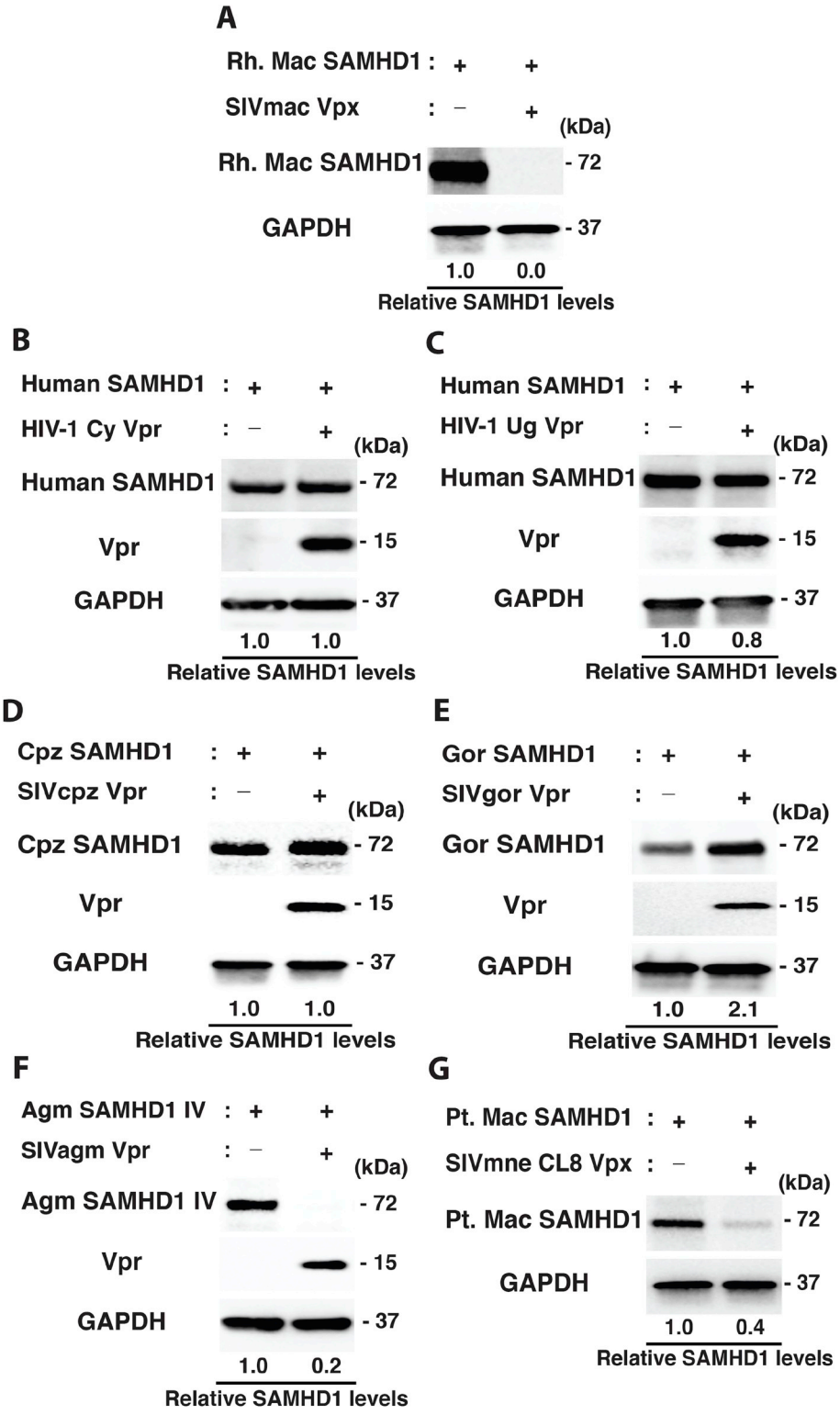

Fig. 1. SAMHD1 degradation capability of primate lentiviruses. SAMHD1 degradation capability by lentiviral proteins was determined using the SAMHD1 degradation assay (Fregoso et al., 2013; Spragg and Emerman, 2013; Mereby et al., 2018). In this assay, 293T cells were co-transfected with a plasmid expressing host specific HA-tagged SAMHD1 proteins (0.1 μg) and a plasmid expressing either flag-tagged or HA-tagged viral accessary proteins (Vpx or Vpr), the entire (SIVmne CL8), or partial viral proteins (SIVmac251) (2 μg). The levels of SAMHD1 were determined by western blots with anti-HA antibody (A, D-G) or *anti*-hSAMHD1 antibody (B and C), and the expression of the viral accessary protein (Vpx or Vpr) were determined by anti-flag tag (SIVagm 9063–2) or anti-HA tag (HIV-1 Cy, HIV-1 Ug, SIVgor, and SIVcpz) antibody. GAPDH was used as a loading control. **(A)** Test for Rhesus macaque (Rh Mac) SAMHD1 degradation by SIVmac251 (−) and (+) Vpx. **(B)** Test for human SAMHD1 degradation by HIV-1 Cy Vpr protein. **(C)** Test for human SAMHD1 degradation by HIV-1 Ug Vpr. **(D)** Test for chimpanzee SAMHD1 degradation by SIVcpz Vpr. **(E)** Test for gorilla SAMHD1 degradation by SIVgor Vpr. **(F)** Test for African green monkey haploid type IV SAMHD1 (Agm SAMHD1 IV) degradation by SIVagm 9063-2 Vpr. **(G)** Test for pig-tail macaque (Pt Mac) SAMHD1 degradation by SIVmne CL8 full length molecular clone. pCDNA3.1-hygro, a plasmid that does not express viral proteins, was used as a negative (−) control in B-G. The molecular weight of each protein presented is marked. The data presented in this figure are representative data from two independent transfections. The mean relative SAMHD1 levels shown were calculated by densitometry analysis and normalized to the GAPDH loading control. The calculated mean ± SD (standard deviation) values corresponding to the normalized SAMHD1 levels following challenge with Vpr/Vpx are (A) 0.024 ± 0.025 (B) 1.042 ± 0.485 (C) 0.766 ± 0.101 and (D) 0.181 ± 0.061 (E) 0.397 ± 0.093 (F) 2.121 ± 0.233 (G) 0.959 ± 0.548.

2013; Spragg and Emerman, 2013; Mereby et al., 2018). The Vpr genes of SIVgor, SIVcpz and SIVagm 9063–2 were expressed in order to observe their ability to mediate the degradation of their host SAMHD1. As a control, Vpx of SIVmac251 (pSIV3) was tested. In the SAMHD1 degradation assay (Fregoso et al., 2013; Spragg and Emerman, 2013; Mereby et al., 2018), 293T cells were co-transfected with a lentiviral plasmid expressing the host SAMHD1 protein and a mammalian plasmid expressing the corresponding Vpr or Vpx protein. SAMHD1 protein levels were monitored by western blots. Vpr, Vpx, and SAMHD1 proteins expressed in this assay were tagged with either HA- or Flag-tag at their N-terminal ends. The ratios of the SAMHD1 protein levels in each of the triplicated SAMHD1 degradation assay were calculated for comparison using densitometry analysis. Since SIVmne CL8 has never been assessed for its ability to degrade SAMHD1, SIVmne CL8 Vpr or Vpx could possess or lack the ability to counteract SAMHD1. For this reason, we utilized a full-length molecular clone of SIVmne CL8, rather than a plasmid containing its Vpr or Vpx protein, to assess the SAMHD1 degradation capabilities of this virus.

First, as shown in Fig. 1A, the level of the rhesus macaque SAMHD1 protein in the transfected 293T cells was markedly reduced when the cells were co-transfected with a SIVmac251 plasmid (pSIVmac + Vpx) that expresses all viral proteins except Env. However, this reduction was not observed when SAMHD1 was co-transfected with the same SIVmac251 plasmid containing a Vpx deletion (pSIVmac -Vpx). However, Vpr proteins of two HIV-1 strains, HIV-1 Cy (Fig. 1B) and HIV-1 Ug (Fig. 1C), could not degrade their host SAMHD1 proteins. In contrast, Vpr of SIVagm 9063–2 (Fig. 1F) degraded African green monkey haplotype IV SAMHD1 protein in this assay. It was previously reported that SIVagm strains from different subspecies of African green monkeys use their Vpr proteins to degrade their host haploid type specific SAMHD1 proteins (Spragg and Emerman, 2013). Also, the transfection of the molecular clone of Vpx-encoding SIVmne CL8 (Fig. 1G) also degraded pig-tail macaque SAMHD1 protein. Importantly, Vpr proteins of both SIVcpz (Fig. 1D) and SIVgor (Fig. 1E) could not degrade their host SAMHD1 proteins. Collectively, the results in Fig. 1 demonstrate that. As is the case for HIV-1, SIVgor and SIVcpz do not degrade their host SAMHD1 protein, whereas SIVagm 9063–2 and SIVmne CL8 proteasomally degrade their host SAMHD1 proteins. Therefore, this data suggests that while SIVgor and SIVcpz should replicate under SAMHD1-mediated limited dNTP pools in macrophages, both SIVagm 9063–2 and SIVmne CL8 should replicate under abundant dNTP conditions even in macrophages.

Pre-steady state kinetic analysis of SIVgor and SIVcpz RTs: The enzymatic dNTP incorporation by DNA polymerases including RTs follows a series of sequential mechanistic steps that can be separately measured for their kinetic rates (Hsieh JC and Modrich, 1993; Kati et al., 1992; Herschlag et al., 1991; Joyce, 2010). Typically, as illustrated in Fig. 2A, first, RT binds to template:primer (T/P, K_D), forming a binary complex (RT:T/P), and this binary complex binds to a dNTP substrate (K_d, dNTP binding affinity), forming ternary complex (RT:T/P:dNTP). Next, the ternary complex will undergo the k_{pol} step, which consists of two sequential sub-steps: 1) a conformational change of the complex (RT*:T/P:dNTP, K_{conf}) followed by 2) a chemistry step (K_{chem}) to complete the phosphodiester bond formation between 3' OH of the primer and α-phosphate of the dNTP substrate. Substrate incorporation is finally followed by the slow release of PP_i product. Single round pre-steady steady state kinetic analysis has been extensively employed to determine the kinetic rate of these individual steps involved dNTP incorporation by DNA polymerases (Lenzi et al., 2015; Hsieh JC and Modrich, 1993; Kati et al., 1992; Herschlag et al., 1991; Joyce, 2010; Einolf and Guengerich, 2001; Schermerhorn and Gardner, 2015).

Previous studies have shown that RTs originating from SAMHD1 non-counteracting HIV-1 strains are characterized by higher k_{pol} than RTs from various SAMHD1-counteracting SIV strains, which suggested that HIV-1 RTs might have evolved to have faster k_{pol} step in order to complete proviral DNA synthesis even in macrophages harboring SAMHD1-mediated low dNTP pools (Lenzi et al., 2015). SIVcpz and SIVgor are the closest relatives of HIV-1 and, particularly, SIVcpz is considered as the origin of HIV-1. In addition, unlike the SAMHD1-counteracting SIV strains that we previously characterized, SIVcpz and SIVgor not only lack Vpx, but their Vpr proteins do not proteasomally degrade their host SAMHD1 proteins (Fig. 1) (Lim et al., 2012). Therefore, we tested whether SIVcpz and SIVgor RTs also have higher dNTP incorporation efficiency (k_{pol}/K_d) and faster k_{pol} rates, compared to the RTs of SAMHD1-counteracting SIVs (SIVagm 9063–2 and SIVmne CL8). We also employed RTs of two HIV-1 strains (HIV-1 Ug and HIV-1 Cy) as comparison controls.

In order to measure the pre-steady state kinetic values of the RT proteins, which requires a single round of incorporation, we first measured the active site concentration of each purified RT enzyme using pre-steady state burst experiments. Pre-steady state burst experiments, which are performed using an excess T/P to RT enzyme, provide a burst amplitude that defines the concentration of active RT:T/P complexes capable of dNTP incorporation (Equation (1), Experimental Procedures) and is followed by a steady-state turnover rate as the product complex is released from the enzyme in the rate limiting step of the dNTP incorporation pathway (Hsieh JC and Modrich, 1993). We observed typical burst kinetics for all six RTs and found they all possessed 20–75% active protein (Fig. 2B–G and Supplemental Fig. 2).

Next, using all six RTs normalized for their active site concentrations, we employed pre-steady state single turnover experiments to determine the kinetic parameters, K_d and k_{pol}, involved in single nucleotide incorporation by these RTs. In single turnover experiments, prebound RT:T/P binary complexes, created by pre-incubating fivefold excess active RT with radiolabeled T/P, are rapidly mixed with $MgCl_2$ and various concentrations of dTTP substrate ranging from 1 to 100 μM for reactions ranging from 0 to 2 s. Every reaction was quenched at its designated time using EDTA. We first determined the rate of single nucleotide incorporation at each substrate concentration (Equation (2), Experimental Procedures). These rates were then plotted against substrate concentration to determine the dNTP binding affinity (K_d), maximum rate of dNTP incorporation (k_{pol}), and the dNTP incorporation efficiency (k_{pol}/K_d) for each enzyme (Equation (3), Experimental Procedures; Supplemental Fig. 3). As summarized in Table 1 and Fig. 3A, both HIV-1 Ug and HIV-1 Cy RTs displayed relatively fast k_{pol} rates of incorporation (HIV-1 Ug: 594.7 s^{-1}, HIV-1 Cy: 139.80 s^{-1}) in comparison to their SIV SAMHD1-counteracting counterparts (SIVagm 9063–2: 42.92 s^{-1}, SIVmneCL8: 68.17 s^{-1}). The relative difference in k_{pol} values between HIV-1 Ug and HIV-1 Cy was interesting to observe. This roughly four-fold difference between the two lentiviral RT k_{pol} values was retained when conducting pre-steady state kinetic analysis of a dCTP incorporation event at a different location along the same primer-template (data not shown). This suggests that the observed difference is not an effect of primer-template sequence, rather a product of RT activity. Amino acid sequence comparisons of HIV-1 Cy and HIV-1 Ug RTs did not reveal any striking differences outside of a number of proline residue variations that might affect overall protein structure. However, of the many residue differences HIV-1 Cy and HIV-1 Ug RTs possess, any of them could play a role in overall protein dynamics during polymerization. Importantly, RTs from SIVgor and SIVcpz also displayed fast k_{pol} values similar to the HIV-1 RTs at 193.10 s^{-1} and 355.70 s^{-1} respectively. Consistent with previous studies, all six RTs displayed similar K_d values during the incorporation of the dTTP substrate. This indicates that all RTs bind the dNTP substrate with similar affinity, whereas the RTs from the SAMHD1 non-counteracting lentiviruses displayed faster k_{pol} values than the RTs of the SAMHD1 counteracting lentiviral origins (Fig. 3A). We were surprised to find the K_d of HIV-1 Ug RT to be relatively high in comparison to that HIV-1 Cy RT. When observing the aforementioned pre-steady state kinetics of a dCTP incorporation event, HIV-1 Ug displayed K_d values similar to that of HIV-1 Cy, suggesting that the elevated K_d value reported here could possibly be an effect of the primer-template sequence (data not shown). In addition, the overall dNTP incorporation efficiency (k_{pol}/K_d, Fig. 3B and Table 1) is 4–6 times higher in the RTs from the SAMHD1 non-counteracting lentiviruses compared to the RTs from the SAMHD1 counteracting lentiviruses. This data supports the idea that the RTs of the SAMHD1 non-counteracting lentiviruses (HIV-1, SIVgor, and SIVcpz) enable these lentiviruses to circumvent the SAMHD1 restriction and to complete the provirial DNA synthesis even in the limited dNTP pools found in nondividing myeloid cells.

Phosphorothioate elemental effect of RTs from SAMHD1 non-counteracting and counteracting primate lentiviruses: The k_{pol} step consists of two sequential sub-steps, 1) conformational change (K_{conf}) and 2) chemistry (K_{chem}). Therefore, we next tested which of these two sub-steps RTs of SAMHD1 non-counteracting lentiviruses evolutionarily honed over time in order to gain a faster k_{pol} step. The phosphorothioate elemental effect has been used to determine whether the chemical step of a polymerization reaction is rate-limiting and is evaluated by comparing the rates of incorporation of the natural dNTP

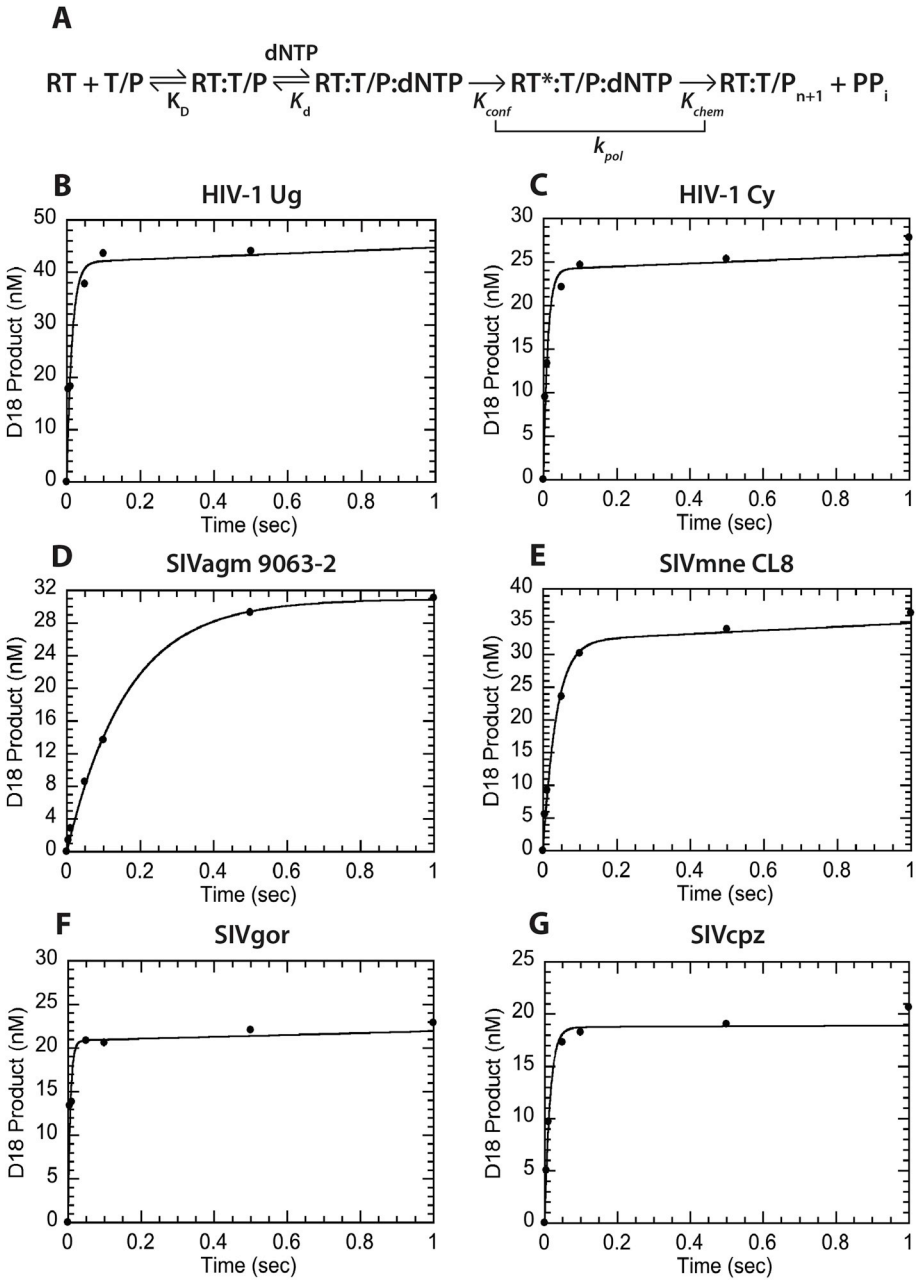

Fig. 2. Determination of active site concentrations of SIVgor and SIVcpz reverse transcriptase proteins by burst kinetic analysis. (A) Scheme for dNTP incorporation by reverse transcriptase (RT). Free RT molecules initially bind to template:primer (T/P, K_D), forming the RT:T/P binary complex. Next, dNTP substrate binds to the binary complex, forming RT:T/P:dNTP ternary complex (K_d, dNTP binding affinity). The ternary complex then undergoes the k_{pol} step which consists of two sequential sub-steps, 1) pre-catalytic conformational change (K_{conf}) forming RT*:T/P:dNTP and 2) chemistry (K_{chem}) extending T/P to T/P $_{n+1}$, followed by the PP$_i$ product release. Burst kinetic analysis of **(B)** HIV-1 Ug, **(C)** HIV-1 Cy, **(D)** SIVagm 9063–2, **(E)** SIVmneCL8, **(F)** SIVgor, and **(G)** SIVcpz RT proteins determined the active site concentration of these proteins. Active site titrations were performed in excess T/P conditions to ensure all RT active sites were occupied by T/P. Substrate (dATP) was added to the reaction to allow single nucleotide incorporation events to occur for 0–3 s. Reaction product was quantified and fit to a burst equation to determine the active site concentration of each RT (Equation (1), Experimental Procedures). Secondary burst kinetic curves for all RTs are shown in Supplemental Fig. 2 to display the range of active site activity for each purified enzyme. Active site concentrations were determined from triplicate experiments for all six RT proteins and the calculated activities were found to range from 20 to 75%.

Table 1
Pre-steady state kinetic values of six primate lentiviral RT proteins with dTTP. Single turnover pre-steady state kinetic analysis was performed using a dTTP substrate. Experiments were conducted in triplicate. Representative plots from which this data derived can be found in Supplemental Fig. 3.

dTTP			
RT strains	k_{pol} (s^{-1})	K_d (μM)	k_{pol}/K_d ($s^{-1} * \mu M^{-1}$)
HIV-1 Ug	594.70 ± 144.00	167.90 ± 69.47	3.71
HIV-1 Cy	139.80 ± 52.40	41.54 ± 21.96	3.58
SIVagm 9063-2	42.92 ± 15.27	40.82 ± 20.63	1.11
SIVmne CL8	68.17 ± 4.46	90.37 ± 37.14	0.83
SIVgor	193.10 ± 77.67	45.21 ± 22.62	5.18
SIVcpz	355.70 ± 83.50	104.50 ± 21.45	3.39

substrate versus a dNTPαS substrate (Equation (4), Experimental Procedures) (Patel et al., 1991; Joyce, 2010). The sulfur on the α-phosphate in dNTPαS significantly slows down the K_{chem} rate, while not affecting K_{conf}. Therefore, if the K_{chem} step is rate limiting, then k_{pol} during the incorporation of dNTPαS also becomes slower than that of the natural dNTP substrate (k_{pol} for dNTPαS is 4–11 times smaller than that for natural dNTPs: elemental effect = 4–11) (Herschlag et al., 1991; Patel et al., 1991; Wong et al., 1991). In contrast, if K_{conf} is the rate limiting and K_{chem} is fast (much smaller than K_{conf} or close to 0), the delayed chemistry step by dNTPαS does not significantly affect the overall k_{pol} step (k_{pol} values for both dNTPs and dNTPαS are similar: elemental effect is less than 4), implying that the k_{pol} rate predominantly represents its pre-catalytic conformational change rate, K_{conf} ($k_{pol} \approx K_{conf}$) (Mizrahi.V et al., 1985; Patel et al., 1991; Joyce, 2010; Polesky AH et al., 1992; Wong I and Johnson, 1991).

To determine whether an elemental effect was present among the six RTs studied here, single turnover experiments were conducted as described above using a dTTPαS substrate and pre-steady state parameters were calculated and compared to those determined with natural dTTP (Table 2; Supplemental Fig. 4) for each RT. As shown in Fig. 4 and Table 2, phosphorophioate elemental effects ($k_{pol}^{dTPP}/k_{pol}^{dTTPαS}$) of all six RT proteins examined in this study were less than 4. The absence of

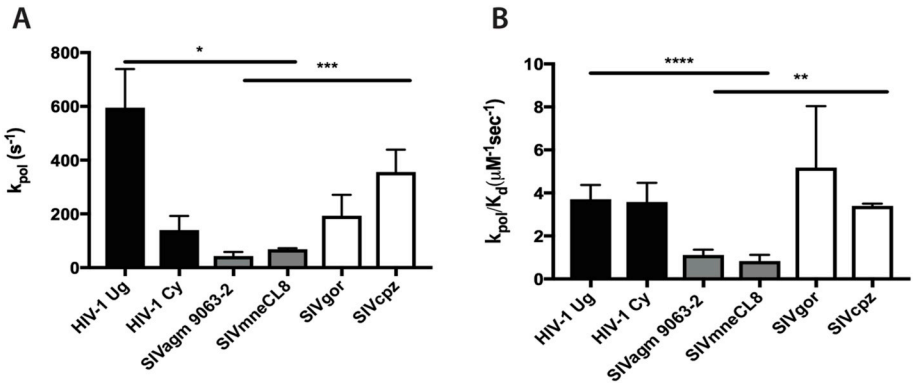

Fig. 3. Comparison of pre-steady state kinetic values among six lentiviral RT proteins. The pre-steady state kinetic k_{pol} and K_d values of HIV-1 Ug, HIV-1 Cy, SIVagm 9063–2, SIVmne CL8, SIVgor, and SIVcpz RT proteins were determined with dTTP (Table 1) as described in Experimental Procedures. Their k_{pol} **(A)** and k_{pol}/K_d **(B)** values were compared. The assays were conducted in triplicate. Statistical significance was determined by first grouping the lentiviral RTs into three groups for comparison: HIV-1 (HIV-1 Cy and HIV-1 Ug), SAMHD1-counteracting SIVs (SIVagm 9063–2 and SIVmne CL8), and SAMHD1 non-counteracting SIVs (SIVgor and SIVcpz). Statistical significance from unpaired two-tailed student's t-tests is indicated as: *, $p < 0.05$; **, $p < 0.01$; ***, $p < 0.001$; ****, $p < 0.0001$.

Table 2
Pres-steady state kinetic values of six primate lentiviral RT proteins with dTTPαS. Single turnover pre-steady state kinetic analysis was performed using a dTTPαS substrate. Experiments were conducted in triplicate. Representative plots from which this data derived can be found in Supplemental Fig. 4.

dTTPαS			
RT strains	k_{pol} (s^{-1})	K_d (μM)	k_{pol}/K_d ($s^{-1} * \mu M^{-1}$)
HIV-1 Ug	182.2 ± 12.22	105.6 ± 16.43	1.74
HIV-1 Cy	140.3 ± 36.36	102.5 ± 66.65	1.69
SIVagm 9063-2	51.11 ± 9.563	114.1 ± 33.35	0.46
SIVmne CL8	50.73 ± 24.43	119.5 ± 41.73	0.41
SIVgor	265.3 ± 92.09	141.8 ± 57.33	1.91
SIVcpz	244.2 ± 163.5	190.5 ± 149.3	1.36

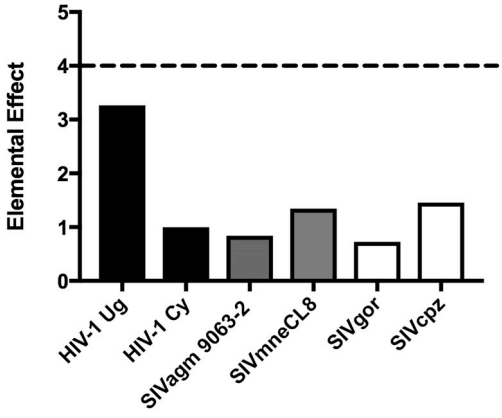

Fig. 4. Phosphorothioate elemental effect of six lentiviral RT proteins. The K_d and k_{pol} values of the six lentiviral RT proteins with dTTP (Table 1) and dTTPαS (Table 2) were determined as described in Experimental procedures, and the phosphorothioate elemental effect of these proteins were calculated as the ratios between mean k_{pol} values with natural dTTP and dTTPαS ($k_{pol}^{dTPP}/k_{pol}^{dTTP\alpha S}$) (Equation (4), Experimental Procedures). An elemental effect value of less than 4 (dotted line) indicates that the conformational change sub-step of the k_{pol} step is rate-limiting (Patel et al., 1991; Wong et al., 1991) and that the pre-catalytic conformational change rate predominantly represents the k_{pol} step in these six RT proteins.

phosphorphioate elemental effect indicates that the conformational change step of these RTs, not their chemistry step, is rate limiting during their overall k_{pol} step, and their k_{pol} values are predominately represented by their conformational change rates. These findings suggest that the faster k_{pol} rate observed with RTs of SAMHD1 non-counteracting lentiviruses (SIVcpz, SIV gor, and HIV-1 strains) is due to their faster rates of the conformational change that occurs post dNTP binding. As illustrated in our model (Fig. 5), while SAMHD1 counteracting lentiviruses (SIVmac239, SIVagm 9063–2, and SIVmne CL8) utilize Vpr/Vpx to counteract SAMHD1 and overcome the kinetic barrier presented in macrophages, our study suggests that SAMHD1 non-counteracting lentiviruses may have evolved over time to harbor RTs that execute a faster conformational change step during nucleotide incorporation, thus enabling the viruses to complete reverse transcription even in the SAMHD1 mediated low dNTP pools of nondividing myeloid cells. In conclusion, while the mechanism employed by SAMHD1 non-counteracting lentiviruses of executing a faster RT conformational change is less effective in overcoming SAMHD1 restriction than the Vpx/Vpr mechanism employed by SAMHD1 counteracting lentiviruses, this RT-based mechanism is sufficient to complete reverse transcription, albeit at slower rates, in the SAMHD1 mediated low dNTP concentrations found in macrophages.

FRET-based measurements have been reported to monitor the post-dNTP binding finger-closing conformational change rate of several DNA polymerases such as DNA polymerase β (Huang et al., 2018) and Klenow fragment of *E. coli* DNA polymerase I (Santoso et al., 2010). However, this type of the measurement has not been fully established for any RT protein. It is possible that this FRET-based assay can be applied for directly comparing the pre-catalytic fingers-closing rates between SAMHD1 counteracting lentiviral RTs and SAMHD non-counteracting lentiviral RTs. There are two potential mechanistic pathways to explain the adaption of the more efficient post dNTP binding conformational change displayed by SAMHD1 non-counteracting lentiviral RTs. First, it is possible that the finger-closing conformational change rates of the SAMHD1 non-counteracting lentiviral RTs are simply faster than those of the SAMHD1 counteracting lentiviral RTs. This possibility can be tested by using the FRET-based assay as described for other DNA polymerases. Second, it is possible that the distance of the movement during the finger-closing conformational change is shorter for the RT proteins of the SAMHD1 non-counteracting lentiviruses, compared to the RT proteins of the SAMHD1 counteracting lentiviruses. This possibility can be investigated through the structural comparison of the ternary complexes of the RT proteins from the SAMHD1 non-counteracting lentiviruses and SAMHD1 counteracting lentiviruses.

Overall, these kinetic studies support the idea that SAMHD1 non-counteracting primate lentiviruses such as HIV-1, SIVgor and SIVcpz might have evolved over time to possess RTs that can more efficiently execute the conformational change step, which enables these lentiviruses to circumvent SAMHD1-mediated dNTP depletion and complete proviral DNA synthesis in nondividing myeloid target cell types.

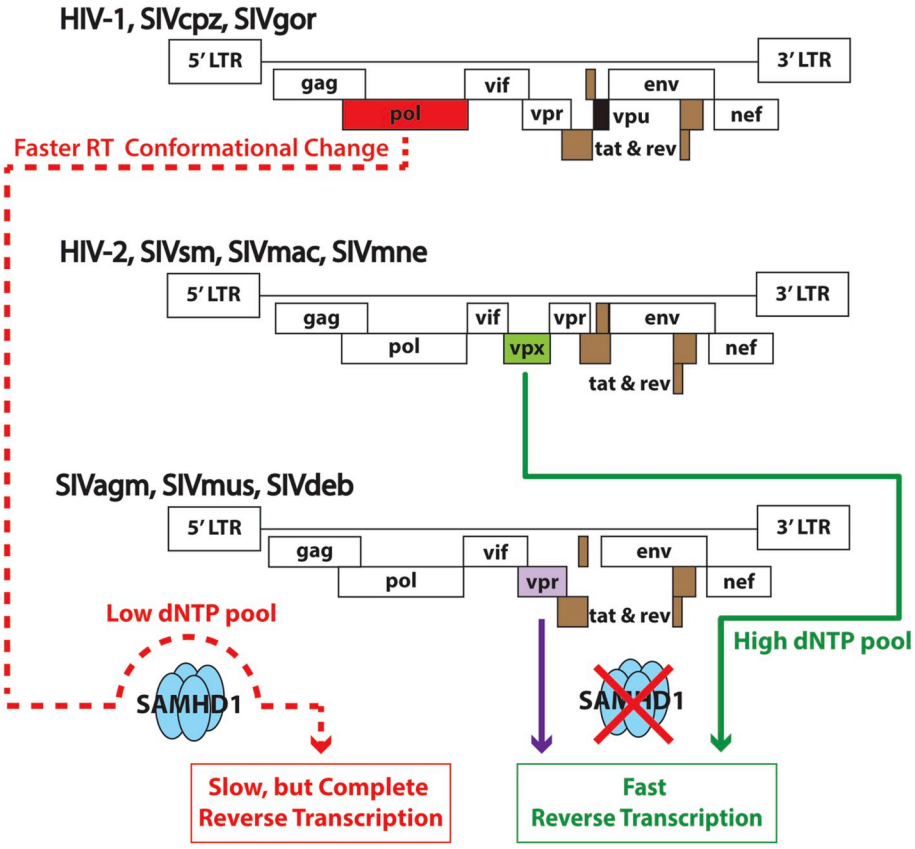

Fig. 5. Model for *anti*-SAMHD1 strategies employed by SAMHD1 non-counteracting and counteracting lentiviruses in non-dividing myeloid cells. In nondividing myeloid cells, while SAMHD1 counteracting viruses utilize Vpx (HIV-2, SIVsm, SIVmac, and SIVmne, green) or Vpr (SIVagm, SIVmus, and SIVdeb, purple) to elevate intercellular dNTP pools and rapidly complete reverse transcription (green and purple lines respectively), SAMHD1 non-counteracting lentiviruses (HIV-1, SIVcpz, and SIVgor) have been evolutionarily honed to perform a faster conformational change step of their RT protein during dNTP incorporation (red dotted line) in order to complete reverse transcription even in the SAMHD1-mediated low dNTP pools. While the mechanism of executing a faster RT conformational change to overcome SAMHD1 restriction is not as effective as the Vpx/Vpr mechanism in overcoming SAMHD1 restriction, it is still sufficient to circumvent (red dotted line) SAMHD1 restriction and complete reverse transcription even at the SAMHD1 mediated low dNTP concentrations found in macrophages. (For interpretation of the references to colour in this figure legend, the reader is referred to the Web version of this article.)

Acknowledgements

This work was supported by NIH AI136581 (B.K.), AI150451 (B.K.), and MH116695 (R.F.S.).

Abbreviations

RT	reverse transcriptase
HIV	human immunodeficiency virus
SIV	simian immunodeficiency virus
SAMHD1	SAM domain and HD domain containing protein 1
Vpx	viral protein X
Vpr	viral protein R
dNTP	deoxynucleoside triphosphate
PP_i	inorganic pyrophosphate

Appendix A. Supplementary data

Supplementary data to this article can be found online at https://doi.org/10.1016/j.virol.2019.08.010.

References

Ahn, J., Hao, C., Yan, J., DeLucia, M., Mehrens, J., Wang, C., Gronenborn, A.M., Skowronski, J., 2012. HIV/simian immunodeficiency virus (SIV) accessory virulence factor Vpx loads the host cell restriction factor SAMHD1 onto the E3 ubiquitin ligase complex CRL4DCAF1. J. Biol. Chem. 287, 12550–12558.

Amie, S.M., Noble, E., Kim, B., 2013. Intracellular nucleotide levels and the control of retroviral infections. Virology 436, 247–254.

Bejarano, D., Puertas, M., Börner, K., Martinez-Picado, J., Müller, B., Kräusslich, H.-G., 2018. Detailed characterization of early HIV-1 replication dynamics in primary human macrophages. Viruses 10, 620.

Belzile, J.P., Duisit, G., Rougeau, N., Mercier, J., Finzi, A., Cohen, E.A., 2007. HIV-1 Vpr-mediated G2 arrest involves the DDB1-CUL4AVPRBP E3 ubiquitin ligase. PLoS Pathog. 3, e85.

Berger, G., Durand, S., Goujon, C., Nguyen, X.N., Cordeil, S., Darlix, J.L., Cimarelli, A., 2011. A simple, versatile and efficient method to genetically modify human monocyte-derived dendritic cells with HIV-1-derived lentiviral vectors. Nat. Protoc. 6, 806–816.

Bhattacharya, A., Wang, Z., White, T., Buffone, C., Nguyen, L.A., Shepard, C.N., Kim, B., Demeler, B., Diaz-Griffero, F., Ivanov, D.N., 2016. Effects of T592 phosphomimetic mutations on tetramer stability and dNTPase activity of SAMHD1 can not explain the retroviral restriction defect. Sci. Rep. 6, 31353.

D'Arc, M., Ayouba, A., Esteban, A., Learn, G.H., Boue, V., Liegeois, F., Etienne, L., Tagg, N., Leendertz, F.H., Boesch, C., Madinda, N.F., Robbins, M.M., Gray, M., Cournil, A., Ooms, M., Letko, M., Simon, V.A., Sharp, P.M., Hahn, B.H., Delaporte, E., Mpoudi Ngole, E., Peeters, M., 2015. Origin of the HIV-1 group O epidemic in western lowland gorillas. Proc. Natl. Acad. Sci. U. S. A. 112, E1343–E1352.

Diamond, T.L., Roshal, M., Jamburuthugoda, V.K., Reynolds, H.M., Merriam, A.R., Lee, K.Y., Balakrishnan, M., Bambara, R.A., Planelles, V., Dewhurst, S., Kim, B., 2004. Macrophage tropism of HIV-1 depends on efficient cellular dNTP utilization by reverse transcriptase. J. Biol. Chem. 279, 51545–51553.

Einolf, H.J., Guengerich, F.P., 2001. Fidelity of nucleotide insertion at 8-oxo-7,8-dihydroguanine by mammalian DNA polymerase delta. Steady-state and pre-steady-state kinetic analysis. J. Biol. Chem. 276, 3764–3771.

Etienne, L., Hahn, B.H., Sharp, P.M., Matsen, F.A., Emerman, M., 2013. Gene loss and adaptation to hominids underlie the ancient origin of HIV-1. Cell Host Microbe 14, 85–92.

Fiala, K.A., Suo, Z., 2004. Mechanism of DNA polymerization catalyzed by Sulfolobus solfataricus P2 DNA polymerase IV. Biochemistry 43, 2116–2125.

Fregoso, O.I., Ahn, J., Wang, C., Mehrens, J., Skowronski, J., Emerman, M., 2013. Evolutionary toggling of Vpx/Vpr specificity results in divergent recognition of the restriction factor SAMHD1. PLoS Pathog. 9, e1003496.

Gao, F., Robertson, D.L., Carruthers, C.D., Morrison, S.G., Jian, B., Chen, Y., Barre-Sinoussi, F., Girard, M., Srinivasan, A., Abimiku, A.G., Shaw, G.M., Sharp, P.M., Hahn, B.H., 1998. A comprehensive panel of near-full-length clones and reference sequences for non-subtype B isolates of human immunodeficiency virus type 1. J. Virol. 72, 5680–5698.

Gao, F., Vidal, N., Li, Y., Trask, S.A., Chen, Y., Kostrikis, L.G., Ho, D.D., Kim, J., Oh, M.-D., Choe, K., Salminen, M., Robertson, D.L., Shaw, G.M., Hahn, B.H., Peeters, M., 2001. Evidence of two distinct subsubtypes within the HIV-1 subtype A radiation. AIDS Res. Hum. Retrovir. 17, 675–688.

Goldstone, D.C., Ennis-Adeniran, V., Hedden, J.J., Groom, H.C., Rice, G.I., Christodoulou, E., Walker, P.A., Kelly, G., Haire, L.F., Yap, M.W., de Carvalho, L.P., Stoye, J.P., Crow, Y.J., Taylor, I.A., Webb, M., 2011. HIV-1 restriction factor SAMHD1 is a deoxynucleoside triphosphate triphosphohydrolase. Nature 480, 379–382.

Herschlag, D., Piccirilli, J.A., Cech, T.R., 1991. Ribozyme-catalyzed and nonenzymic reactions of phosphate diesters: rate effects upon substitution of sulfur for a nonbridging phosphoryl oxygen atom. Biochemistry 30, 4844–4854.

Hirsch, V.M., Dapolito, G., Johnson, P.R., Elkins, W.R., London, W.T., Montali, R.J., Goldstein, S., Brown, C., 1995. Induction of AIDS by simian immunodeficiency virus

from an African green monkey: species-specific variation in pathogenicity correlates with the extent of in vivo replication. J. Virol. 69, 955–967.
Hollenbaugh, J.A., Montero, C., Schinazi, R.F., Munger, J., Kim, B., 2016. Metabolic profiling during HIV-1 and HIV-2 infection of primary human monocyte-derived macrophages. Virology 491, 106–114.
Hrecka, K., Gierszewska, M., Srivastava, S., Kozaczkiewicz, L., Swanson, S.K., Florens, L., Washburn, M.P., Skowronski, J., 2007. Lentiviral Vpr usurps Cul4-DDB1[VprBP] E3 ubiquitin ligase to modulate cell cycle. Proc. Natl. Acad. Sci. U. S. A. 104, 11778–11783.
Hrecka, K., Hao, C., Gierszewska, M., Swanson, S.K., Kesik-Brodacka, M., Srivastava, S., Florens, L., Washburn, M.P., Skowronski, J., 2011. Vpx relieves inhibition of HIV-1 infection of macrophages mediated by the SAMHD1 protein. Nature 474, 658–661.
Hsieh JC, Z.S., Modrich, P., 1993. Kinetic mechanism of the DNA-dependent DNA polymerase activity of human immunodeficiency virus reverse transcriptase. J. Biol. Chem. 268, 24607–24613.
Huang, J., Alnajjar, K.S., Mahmoud, M.M., Eckenroth, B., Doublie, S., Sweasy, J.B., 2018. The nature of the DNA substrate influences pre-catalytic conformational changes of DNA polymerase beta. J. Biol. Chem. 293, 15084–15094.
Jamburuthugoda, V.K., Chugh, P., Kim, B., 2006. Modification of human immunodeficiency virus type 1 reverse transcriptase to target cells with elevated cellular dNTP concentrations. J. Biol. Chem. 281, 13388–13395.
Johnson, K.A., 1995. Rapid quench kinetic analysis of polymerases, adenosinetriphosphatases, and enzyme intermediates. Methods Enzymol. 249, 38–61.
Joyce, C.M., 2010. Techniques used to study the DNA polymerase reaction pathway. Biochim. Biophys. Acta 1804, 1032–1040.
Kati, W.M., Johnson, K.A., Jerva, L.F., Anderson, K.S., 1992. Mechanism and fidelity of HIV reverse transcriptase. J. Biol. Chem. 267, 25988–25997.
Kim, B., 1997. Genetic selection in Escherichia coli for active human immunodeficiency virus reverse transcriptase mutants. Methods 12, 318–324.
Laguette, N., Sobhian, B., Casartelli, N., Ringeard, M., Chable-Bessia, C., Segeral, E., Yatim, A., Emiliani, S., Schwartz, O., Benkirane, M., 2011. SAMHD1 is the dendritic- and myeloid-cell-specific HIV-1 restriction factor counteracted by Vpx. Nature 474, 654–657.
Lahouassa, H., Daddacha, W., Hofmann, H., Ayinde, D., Logue, E.C., Dragin, L., Bloch, N., Maudet, C., Bertrand, M., Gramberg, T., Pancino, G., Priet, S., Canard, B., Laguette, N., Benkirane, M., Transy, C., Landau, N.R., Kim, B., Margottin-Goguet, F., 2012. SAMHD1 restricts the replication of human immunodeficiency virus type 1 by depleting the intracellular pool of deoxynucleoside triphosphates. Nat. Immunol. 13, 223–228.
Lenzi, G.M., Domaoal, R.A., Kim, D.H., Schinazi, R.F., Kim, B., 2014. Kinetic variations between reverse transcriptases of viral protein X coding and noncoding lentiviruses. Retrovirology 11, 111.
Lenzi, G.M., Domaoal, R.A., Kim, D.H., Schinazi, R.F., Kim, B., 2015. Mechanistic and kinetic differences between reverse transcriptases of vpx coding and non-coding lentiviruses. J. Biol. Chem. 290, 30078–30086.
Lim, Efrem S., Fregoso, Oliver I., McCoy, Connor O., Matsen, Frederick A., Malik, Harmit S., Emerman, M., 2012. The ability of primate lentiviruses to degrade the monocyte restriction factor SAMHD1 preceded the birth of the viral accessory protein vpx. Cell Host Microbe 11, 194–204.
Mangeot, P.E., Negre, D., Dubois, B., Winter, A.J., Leissner, P., Mehtali, M., Kaiserlian, D., Cosset, F.L., Darlix, J.L., 2000. Development of minimal lentivirus vectors derived from simian immunodeficiency virus (SIVmac251) and their use for gene transfer into human dendritic cells. J. Virol. 74, 8307–8315.
Mereby, S.A., Maehigashi, T., Holler, J.M., Kim, D.H., Schinazi, R.F., Kim, B., 2018. Interplay of ancestral non-primate lentiviruses with the virus-restricting SAMHD1 proteins of their hosts. J. Biol. Chem. 293, 16402–16412.
MizrahiV, H.R., Marlier, J.F., Johnson, K.A., Benkovic, S.J., 1985. Rate-limiting steps in the DNA polymerase I reaction pathway. Biochemistry 24, 4010–4018.
Patel, S.S., Wong, I., Johnson, K.A., 1991. Pre-steady-state kinetic analysis of processive DNA replication including complete characterization of an exonuclease-deficient mutant. Biochemistry 30, 511–525.
Polesky AH, D.M., Benkovic, S.J., Grindley, N.D., Joyce, C.M., 1992. Side chains involved in catalysis of the polymerase reaction of DNA polymerase I from Escherichia coli. J. Biol. Chem. 267, 8417–8428.
Reardon, J.E., 1992. Human immunodeficiency virus reverse transcriptase: steady-state and pre-steady-state kinetics of nucleotide incorporation. Biochemistry 31, 4473–4479.
Rudensey, L.M., Kimata, J.T., Benveniste, R.E., Overbaugh, J., 1995. Progression to AIDS in macaques is associated with changes in the replication, tropism, and cytopathic properties of the simian immunodeficiency virus variant population. Virology 207, 528–542.
Sakai, Y., Doi, N., Miyazaki, Y., Adachi, A., Nomaguchi, M., 2016. Phylogenetic insights into the functional relationship between primate lentiviral reverse transcriptase and accessory proteins vpx/vpr. Front. Microbiol. 7, 1655.
Santoso, Y., Joyce, C.M., Potapova, O., Le Reste, L., Hohlbein, J., Torella, J.P., Grindley, N.D., Kapanidis, A.N., 2010. Conformational transitions in DNA polymerase I revealed by single-molecule FRET. Proc. Natl. Acad. Sci. U. S. A. 107, 715–720.
Schermerhorn, K.M., Gardner, A.F., 2015. Pre-steady-state kinetic analysis of a family D DNA polymerase from thermococcus sp. 9 degrees N reveals mechanisms for archaeal genomic replication and maintenance. J. Biol. Chem. 290, 21800–21810.
Schwefel, D., Groom, H.C., Boucherit, V.C., Christodoulou, E., Walker, P.A., Stoye, J.P., Bishop, K.N., Taylor, I.A., 2014. Structural basis of lentiviral subversion of a cellular protein degradation pathway. Nature 505, 234–238.
Sharp, P.M., Bailes, E., Stevenson, M., Emerman, M., Hahn, B.H., 1996. Gene acquisition in HIV and SIV. Nature 383, 586–587.
Skasko, M., Weiss, K.K., Reynolds, H.M., Jamburuthugoda, V., Lee, K., Kim, B., 2005. Mechanistic differences in RNA-dependent DNA polymerization and fidelity between murine leukemia virus and HIV-1 reverse transcriptases. J. Biol. Chem. 280, 12190–12200.
Skasko, M., Diamond, T.L., Kim, B., 2009. Mechanistic variations among reverse transcriptases of simian immunodeficiency virus variants isolated from African green monkeys. Biochemistry 48, 5389–5395.
Spragg, C.J., Emerman, M., 2013. Antagonism of SAMHD1 is actively maintained in natural infections of simian immunodeficiency virus. Proc. Natl. Acad. Sci. U. S. A. 110, 21136–21141.
Srivastava, S., Swanson, S.K., Manel, N., Florens, L., Washburn, M.P., Skowronski, J., 2008. Lentiviral Vpx accessory factor targets VprBP/DCAF1 substrate adaptor for cullin 4 E3 ubiquitin ligase to enable macrophage infection. PLoS Pathog. 4, e1000059.
Swanstrom, A.E., Del Prete, G.Q., Deleage, C., Elser, S.E., Lackner, A.A., Hoxie, J.A., 2018. The SIV envelope glycoprotein, viral tropism, and pathogenesis: novel insights from nonhuman primate models of AIDS. Curr. HIV Res. 16, 29–40.
Takehisa, J., Kraus, M.H., Decker, J.M., Li, Y., Keele, B.F., Bibollet-Ruche, F., Zammit, K.P., Weng, Z., Santiago, M.L., Kamenya, S., Wilson, M.L., Pusey, A.E., Bailes, E., Sharp, P.M., Shaw, G.M., Hahn, B.H., 2007. Generation of infectious molecular clones of simian immunodeficiency virus from fecal consensus sequences of wild chimpanzees. J. Virol. 81, 7463–7475.
Takehisa, J., Kraus, M.H., Ayouba, A., Bailes, E., Van Heuverswyn, F., Decker, J.M., Li, Y., Rudicell, R.S., Learn, G.H., Neel, C., Ngole, E.M., Shaw, G.M., Peeters, M., Sharp, P.M., Hahn, B.H., 2009. Origin and biology of simian immunodeficiency virus in wild-living western gorillas. J. Virol. 83, 1635–1648.
Weissman, D., Rabin, R.L., Arthos, J., Rubbert, A., Dybul, M., Swofford, R., Venkatesan, S., Farber, J.M., Fauci, A.S., 1997. Macrophage-tropic HIV and SIV envelope proteins induce a signal through the CCR5 chemokine receptor. Nature 389, 981–985.
Williams, K.C., Hickey, W.F., 2002. Central nervous system damage, monocytes and macrophages, and neurological disorders in AIDS. Annu. Rev. Neurosci. 25, 537–562.
Wong, I., Patel, S.S., Johnson, K.A., 1991. An induced-fit kinetic mechanism for DNA replication fidelity: direct measurement by single-turnover kinetics. Biochemistry 30, 526–537.
Wong I, P.S., Johnson, K.A., 1991. An induced-fit kinetic mechanism for DNA replication fidelity: direct measurement by single-turnover kinetics. Biochemistry 30, 526–537.
Yu XF, Y.Q., Essex, M., Lee, T.H., 1991. The vpx gene of simian immunodeficiency virus facilitates efficient viral replication in fresh lymphocytes and macrophage. J. Virol. 65, 5088–5091.
Zahurancik, W.J., Klein, S.J., Suo, Z., 2013. Kinetic mechanism of DNA polymerization catalyzed by human DNA polymerase epsilon. Biochemistry 52, 7041–7049.
Zhou, X., DeLucia, M., Hao, C., Hrecka, K., Monnie, C., Skowronski, J., Ahn, J., 2017. HIV-1 Vpr protein directly loads helicase-like transcription factor (HLTF) onto the CRL4-DCAF1 E3 ubiquitin ligase. J. Biol. Chem. 292, 21117–21127.